OCEANOGRAPHY

High sea surface temperatures were a prerequisite for the development and expansion of the Great Barrier Reef

Benjamin Petrick[1]*, Lars Reuning[1], Alexandra Auderset[2], Miriam Pfeiffer[1], Gerald Auer[3], Lorenz Schwark[1,4]

The Great Barrier Reef is the largest reef system in the modern ocean. To date, the influence of temperature on the origin and long-term evolution of the Great Barrier Reef remains enigmatic. Here, we present a 900–thousand year TEX_{86}^{H}-derived temperature proxy record from Ocean Drilling Program Site 820 in the Coral Sea. It demonstrates that the onset of reef growth on the outer shelf was preceded by a rise in summer temperature from ~26° to ~28°C at around 700 thousand years ago (marine isotope stage 17). This approximately 2°C rise in summer sea surface temperatures (SSTs) likely resulted in higher carbonate production rates, which were crucial for the formation of the Great Barrier Reef. Subsequently, reconstructed SSTs remained sufficiently warm for the Great Barrier Reef to thrive and evolve continuously. The evolution of the Great Barrier Reef, therefore, appears to be closely linked to SSTs.

INTRODUCTION

The Great Barrier Reef (GBR), a UNESCO World Heritage Site (Fig. 1), is by far the largest barrier reef system in the world today (*1*), being more than 300 times larger than the second largest barrier reef off the coast of Belize (*2*, *3*). The onset of the GBR evolution is debated and was initially thought to have been between 900 and 400 thousand years ago (ka) (*4*). An alkenone (U^{K}_{37}')–based sea surface temperature (SST) reconstruction covering the last 800 thousand years (kyr) shows only low-amplitude SST changes and, therefore, does not support a link between changing SST and the development of the GBR (*5*). This led authors to suggest that SST played only a minor to no role in the development of the GBR (*5*–*7*). However, more recent reconstructions from the Coral Sea suggest higher-magnitude glacial to interglacial SST changes based on element ratios measured on foraminifers and coral skeletons (*8*–*11*). Therefore, improved paleo-SST records of past climate changes are critical to understanding the role of temperature in the establishment and climate-driven responses of the GBR ecosystem.

Here, we use TEX_{86}^{H}, an SST proxy based on the cyclization of GDGTs (glycerol dialkyl glycerol tetraethers), to reconstruct SST changes over the last ~900 kyr from Ocean Drilling Program (ODP) Site 820 in the Coral Sea, only 8 km off the edge of the GBR (Fig. 1). With these data, we provide a long-term record of SST and can place the development of the GBR in the Pleistocene in the context of regional climatic changes.

RESULTS

Holocene TEX_{86}^{H}-derived SST at ODP Site 820 represents temperatures that are 2.0°C warmer than annually averaged SSTs and closer to modern summer SST. For more information, see the Supplementary Materials. Reconstructed summer SSTs across the entire record average 27.3°C (Fig. 2). The warmest point was 30.0°C during marine isotope stage (MIS) 5, and the coldest was 24.3°C during MIS 12. Before MIS 17, SSTs were as low as 24.5°C and did not exceed 28.1°C (Fig. 2). Then, between MIS 17 and MIS 13, temperatures ranged between 26° and 29°C, followed by a final cooling to 24.3°C during MIS 12 (Fig. 2). After MIS 12, high interglacial temperatures reached 30.0°C, and glacial SSTs stayed above 26.0°C, except for MIS 4 when temperatures were around 25.5°C. Our record shows a higher SST range than a previously published U^{K}_{37}'-based SST-proxy dataset (*5*) (see the Supplementary Materials for a detailed discussion). In contrast, the TEX_{86}^{H} record agrees with the 3° to 4°C glacial to interglacial temperature increases seen in the foraminiferal Mg/Ca-based (*10*–*12*) and the coral Sr/Ca-based SST-proxy records (*8*, *9*) from the Coral Sea (fig. S1).

DISCUSSION

The most important difference between the GBR and other modern coral reef systems is its large spatial extent compared to other coral reef systems (*2*, *3*). Its development would have required prolonged periods of time with very high carbonate production rates. SST is the major factor controlling the carbonate production of tropical coral reef systems (*13*). Optimum conditions for coral carbonate production are close to their upper thermal limit (*14*). This explains the apparent contradiction between the high carbonate production of coral reefs in the warmest ocean waters (*15*–*17*) and their sensitivity to short-term thermal stress bleaching events that currently increase in frequency due to global warming. Warmer SSTs support higher coral growth and carbonate production rates in tropical reef systems (*17*, *18*). This temperature dependence has been demonstrated in numerous studies investigating major reef-building corals from the GBR, which show an increase in growth and calcification rates with increasing SSTs (*16*, *19*, *20*). Well-dated Holocene reef cores also show higher reef accretion rates in warmer climates during the Early to Middle Holocene in all tropical oceans (*21*). Summer temperatures above 24°C are a lower limit for the proliferation of tropical coral reef platforms (*13*, *18*), although reefs can persist in areas where winter temperatures stay above 18°C.

[1]Christian-Albrechts-Universität zu Kiel, Institute of Geosciences, Kiel, Germany. [2]Department of Ocean and Earth Science, University of Southampton, Southampton, UK. [3]Department of Earth Sciences, NAWI Graz Geocenter, University of Graz, Graz, Austria. [4]WA-OIG, School of Earth and Planetary Sciences, Curtin University, Perth, Australia.
*Corresponding author. Email: benjamin.petrick@ifg.uni-kiel.de

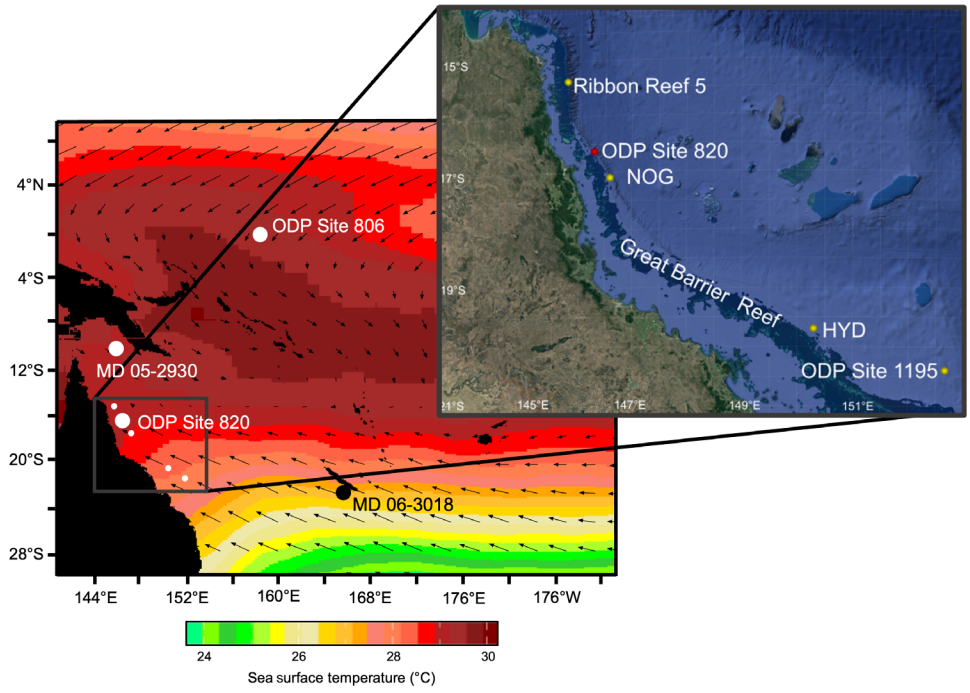

Fig. 1. Maps showing the GBR and core sites that are discussed in this article. The zoomed-out map shows the modern surface winds (arrows) and sea surface austral summer temperatures (colors) for February in the SW-Pacific. SST data are taken from NOAA Optimal Interpolation SST (*28*), and wind data are taken from the NCEP/NCAR 40 reanalysis (*54*). Charts computed at IRI/LDEO Climate Data Library (http://iridl.ldeo.columbia.edu; date accessed: 25 May 2023). The locations of the sites mentioned in the text and supplements are indicated: ODP Site 806 (*55*), MD 05-2930 (*11*), and MD 06-3018 (*12*). Zoomed-in map showing that GBR was generated using Google Earth (*56*). The locations of the sites mentioned in the text and supplements are indicated: ODP Site 1195 (*7*), Ribbon Reef 5 (*22*), NOG (Noggin Pass), and HYD (Hydrographer's Passage) from Integrated Ocean Drilling Project (IODP) Expedition 325 (*8*, *9*).

Because of the importance of SSTs to carbonate production and reef development, we compared our SST data to an existing record of Pleistocene coral reef development, the Ribbon Reef 5 borehole (*22*–*24*) (Fig. 2). A major change in coral community structure and the beginning of a cyclic repetition in coral assemblages starting at 137 m marks the establishment of a barrier reef system at the outer shelf (*25*) (Fig. 2). A radiogenic uranium/thorium decay date of 616±51 ka at 118 m (*26*) indicates a minimum age of MIS 15 for this reef section. The depth of 137 m in the core was tentatively assigned to MIS 17 (Fig. 2) (*23*). This timing matches changes in sedimentology at Site 820. The carbonate content (*27*) rapidly increased from 900 ka (MIS 22) to 700 ka (MIS 17), indicating a reduction in terrestrial input during this time (Fig. 2). In the southern GBR at ODP Site 1195, a similar change in lithology has been interpreted as indicating the initiation of the GBR between ~560 and 670 ka (MIS 15 or 17) and the consequent retention of terrestrial input inshore of this topographic barrier (*7*). Together with evidence from the Ribbon Reef core, MIS 17 seems to mark a major step in the development of the GBR.

Overall, before ~700 ka (MIS 17), we detect a steeper SST gradient to ODP Site 806 in the Western Pacific Warm Pool (WPWP), suggesting subtropical conditions at Site 820 (Fig. 2B). All glacial summer SSTs were at or below 26°C, with minima <25°C during MIS 18, MIS 20, and MIS 22. Assuming a modern seasonality of ~5°C (*28*), this would indicate winter temperatures of ~20°C. Temperatures below the threshold of 24°C during large parts of the year likely resulted in low rates of tropical carbonate production (*13*, *18*) and coral growth and calcification (*16*, *20*). The consequent low coral reef accretion potential would have left the reefs susceptible to other stressors, such as rapid relative sea level rise or siliciclastic input (*29*). The environmental conditions during the period before 700 ka appear to have been unfavorable for the expansion of existing small reefs into the vast barrier system of the GBR. We, therefore, interpret the shift toward ~2°C higher temperatures after ~700 ka (Fig. 2A) as a critical step for the formation of the GBR.

Even after the "establishment" of the barrier system during the early reef cycles between 137 and 85 m (Cy7 and Cy8, respectively, in Fig. 2), there is a lack of reef framework, suggesting that the GBR was still in its infancy (*25*). On the basis of the age model presented in (*26*), the upper end of this interval can be assigned to MIS 13 (Fig. 2). Between the start of MIS 17 and the end of MIS 13, SSTs remained between 26° and 30°C, which is close to the modern summer SSTs in the Coral Sea (*30*), and glacial-interglacial amplitudes remained <2.5°C (Fig. 2A). The first indication of abundant in situ reef framework at 85 m (*25*) at the Ribbon Reef 5 borehole can be placed at MIS 13 (Fig. 2) according to available age constraints (*23*, *26*). The global $\delta^{18}O$ stack indicates relatively low amplitude sea level fluctuations during this time (*31*). This extended stable period of warmth and relatively stable sea level matches the period of barrier reef development at the Ribbon Reef 5 site (*25*) (Fig. 2E). Our record suggests that the SST between MISs 17 and 13 in the central GBR was ideal for allowing a barrier reef system to develop over several glacial/interglacial cycles. One important difference between the GBR and other modern coral reef systems is its size and complexity. Therefore, the relatively stable and warm SST may be one of the key drivers in forming a coral barrier reef system as big and complex as the GBR.

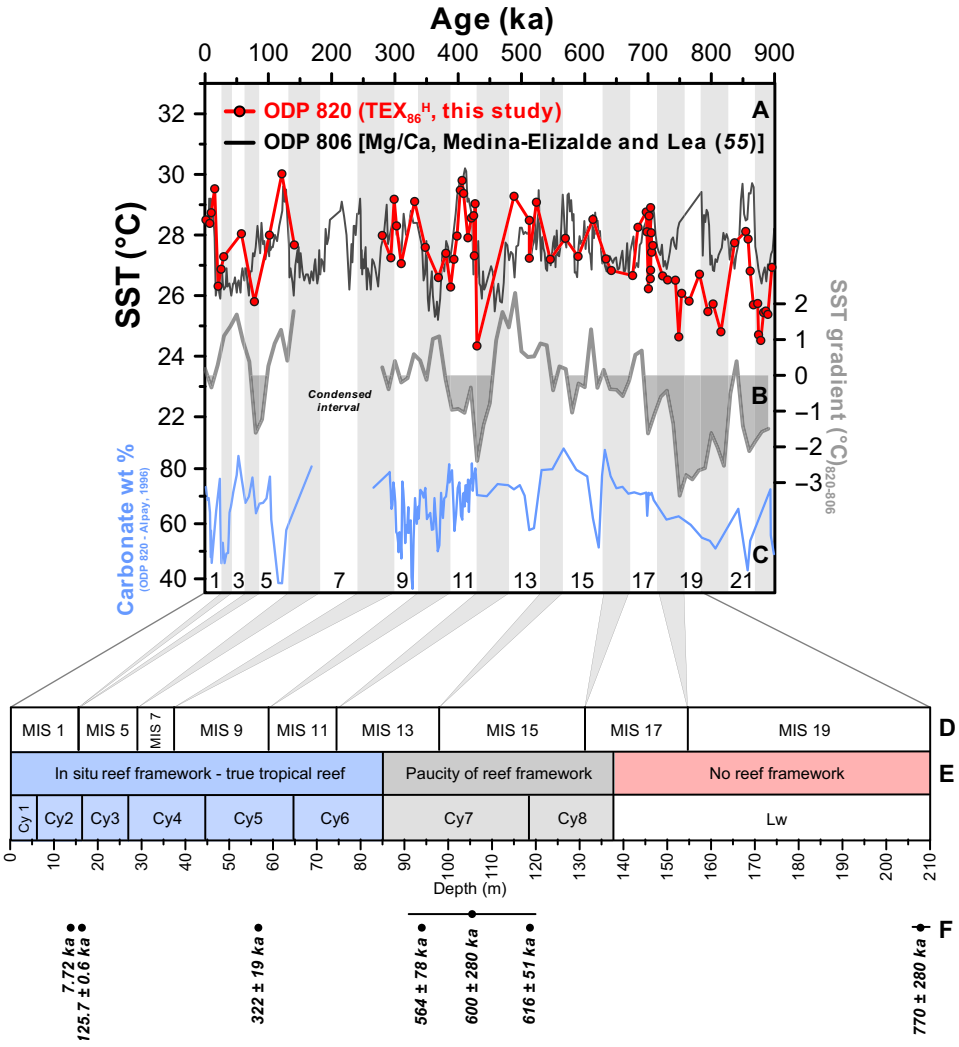

Fig. 2. ODP 820 TEX_{86}^{H}-derived SST record correlated with major events in the development of the GBR based on the Ribbon Reef 5 borehole. (**A**) ODP 820 TEX_{86}^{H} (16.64°S, 146.30°E). Summer SST record (red) compared to the annual average Mg/Ca-SST record of ODP 806 (0.32°N, 159.36°E) (*55*), gray-white banding within (A) delineates the MIS related to glacial (even MIS, gray) and interglacials (uneven MIS, white), (**B**) SST gradient between ODP Sites 820 and 806 with resampled Mg/Ca-SST time series to match the resolution of the TEX_{86}^{H} data. (**C**) ODP Site 820 carbonate content (wt %) based on XRD [blue (*27*)]. (**D**) Proposed MISs for the Ribbon Reef 5 borehole (15.37°S, 145.79°E) (*23*). (**E**) Interpretation of coral reef development from the Ribbon Reef 5 borehole. Cy1 to Cy8 indicate the different reef cycles. Lw stands for the lower unit without shallow-water reef framework (*25*). (**F**) Age data reported for the Ribbon Reef 5 borehole (*26*).

After MIS 17, a connection between SSTs at ODP Site 820 and the WPWP is noted (Fig. 2B). Today, most of the Coral Sea's water derives from the Central Pacific. However, during austral summer, there is a stronger connection to the WPWP as it expands southward (Fig. 1). This is also driven by the southward migration of the Intertropical Convergence Zone (ITCZ), which drives warm water from the central Pacific into the Coral Sea. It is well known that the ITCZ shifts southward during colder climates (*32*, *33*). Given that our summer SST reconstruction reflects warmer SSTs during this period, the most likely explanation is that MIS 17 marks a southward expansion of the WPWP, at least during the summers (Fig. 2B). This fits with evidence finding a southward shift in the ITCZ and the WPWP during the Mid Pleistocene Transition (*12*, *34*). This shift is at its most southward limit between 800 and 500 ka, consistent with the MIS 17 to 13 period showing the most stable SSTs (*34*). Last, work on the west coast of Australia shows that changes in sea level increasingly affected the Indonesian Throughflow, also during MIS 17 (*35*, *36*). It is possible that the greater exposure of the Maritime Continent due to sea level drops might have played a role in shifting the ITCZ further south during glacials at this period (*37*). However, there is a lack of records over this period of time to fully address the wider climatic and oceanographic changes for the Coral Sea around MIS 17. Therefore, this finding may help to understand one of the key questions: Why did the GBR flourish during the large glacial/interglacial cycles of the 100 ka world? The answer from our data is that a stable WPWP and southward-shifted ITCZ kept SSTs warm, providing ideal conditions for reef growth and development between MIS 17 and 13, even during glacials, which would have allowed the active expansion of the GBR even during less favorable climate regimes.

This pattern continues in MIS 11 (424 to 374 ka). MIS 11 is often considered one of the longest and warmest interglacials of the

Middle to Late Pleistocene (*38*, *39*). It has been suggested that this extended period of warmth and higher sea levels led to the establishment of the GBR (*40*). This was previously rejected because SST data did not show a particularly warm interglacial (*5*, *6*, *25*). MIS 11 in the ODP 820 TEX_{86}^{H} record, though not the warmest interglacial, is the first of the interglacials to have summer SST near 30°C (Fig. 2). Our records, therefore, confirm that MIS 11 probably represents an important time for the expansion of the GBR due to its warmth and high sea level.

Because of the sea level fall during the LGM, the coral reef system was forced to migrate to the edge of the existing reef platform, and it can be assumed that a similar process happened during earlier glacials (*29*, *41*). The glacials preserved in the record after MIS 11 continue to show summer SST at or above ~26°C (Fig. 2). Glacial summer SST above 26°C would have allowed coral larvae to establish these low-stand reefs during the glacials (*42*), which could then repopulate the shelf when sea levels rose again, allowing the system to survive multiple glacial cycles (*9*, *12*, *25*, *41*). It is also possible that the higher-amplitude sea level changes, coupled with the warmer stable SSTs, aided in the development of the in situ reef framework of the GBR system, as previously suggested (*25*). In summary, our data suggest that the conditions after MIS 11 continued to be ideal for the growth of the GBR.

In addition, other processes may have contributed to the development of the GBR on glacial to interglacial timescales. First, sea level change is an important controlling factor for the internal architecture of the GBR, as it defines the location of the reef belts between glacial and interglacial periods (*29*). The increase in the amplitude of sea level fluctuations throughout the Middle Pleistocene potentially also influenced the reef-coral community structure of the GBR, which changed toward faster-growing acroporids capable of keeping up with fast-paced sea level changes (*25*, *41*). In addition, sea level influences the input of terrestrial sediments and nutrients to the GBR, which has been shown to influence reef development (*29*, *43*, *44*).

Last, the influence of siliciclastic input on the development of the GBR has been investigated best on glacial-interglacial and shorter timescales, but one study links the original formation of the GBR with the contemporaneous formation of Fraser Island (K'gari) (*6*). The authors argue that the development of Fraser Island would have strongly reduced the sediment supply to the continental shelf north of the island, facilitating widespread coral reef formation in the southern and central GBR area (*6*). They reinterpret the observed decrease in siliciclastic input at Site 1195 at ~700 ka as evidence for this process rather than as an effect of sediment trapping behind the developing barrier reef as initially interpreted (*7*). However, the fact that a similar decrease in siliciclastic input can be observed at Site 820, more than 1100 km north of Fraser Island at about the same time (Fig. 2), makes it unlikely that the formation of Fraser Island alone is responsible for this process. We cannot rule out that the formation of Fraser Island influenced the development of the southern part of the GBR. However, we propose that the observed temperature rise around 700 ka (Fig. 2A) was the decisive factor in initiating the formation of the world's largest barrier reef system.

Consequently, our data suggest that extended periods of optimal temperatures are a prerequisite for the development and maintenance of the GBR. At present, heat waves associated with global warming have caused widespread coral bleaching and are a major threat to the survivability of coral reefs (*45*, *46*). It has been suggested that warming-induced range expansion of tropical corals into subtropical latitudes may provide crucial climate change refuges (*47*, *48*). However, reefs at subtropical latitudes are under an increased risk of marine cold spells causing massive coral bleaching events (*49*). Such extreme cold events will persist or even increase in the future, especially at middle to high latitudes (*50*, *51*). Even today, cold spells are an important limiting factor for the range expansion of reef-building coral taxa, highlighting the particularly narrow temperature field necessary for the proliferation of corals and the proliferation of reef ecosystems.

In conclusion, we show an unequivocal link between SST and the establishment of the GBR. Before ~700 ka, relatively cold SSTs allowed reefs to persist, but they were not able to accrete into a large barrier reef system. The ~2°C increase in summer SST after ~700 ka led to an increase in carbonate production rates and the consequent establishment of the GBR. Since then, our data show that warm SST linked to the WPWP might have played a key role in allowing the reef system to survive the glacial periods when the SST remained sufficiently warm to establish productive coral reefs in low–sea level refugia. Warm and stable SST between MIS 17 and MIS 13 may have favored the development of an extensive barrier reef system. Warm glacials allowed for a rapid reestablishment of the reef during the beginning of interglacials. Therefore, although our results may seem contrary to the current situation of global warming, they nevertheless offer important insights into the stringent temperature confines dictating the capability for coral reefs to proliferate.

MATERIALS AND METHODS

For this study, we collected 88 samples from ODP Site 820 covering the past 900 kyr. Initial sampling was guided by the existing $\delta^{18}O$ record to choose samples at glacial and interglacial maxima and minima. We took samples at higher resolution over key intervals critical for the onset of the GBR, including the last deglaciation, MIS 11, and the period between MIS 18 and 13. Last, once the increasing temperatures around MIS 17 became evident, we took additional samples to confirm this trend and increase the sampling resolution of the pre–MIS 17 glacials. The samples were freeze dried and analyzed for biomarkers in the organic geochemistry laboratory at Kiel University.

For this project, we took 30 cm^3 of sediment, leading to between 30 and 40 g of sediment extracted. Pilot work showed that due to low extract yields, large-volume sampling was essential to obtain sufficient amounts of GDGT lipids for the determination of the TEX_{86}^{H} paleo SST proxy. Samples were Soxhlet extracted for 48 hours using a solvent mixture of DCM:MeOH (9:1, v/v). Elemental sulfur was removed by the addition of activated copper turnings. Excess solvent was evaporated by a Büchi solvent evaporator to a final volume of 2 ml, and samples were then transferred into a 4-ml vial, where the total extract (TE) was taken to dryness under a gentle stream of nitrogen. TEs were fractionated into aliphatic, aromatic, and polar fractions by silica gel-column chromatography (6 ml of SPE column, 2.8 g of Silica 60 mesh, 25 to 40 μm) using solvents with increasing polarity in an LC-TECH automated SPE system. Nitrogen, sulfur, and oxygen (polar) compounds were eluted with 14 ml of DCM/MeOH (1:1, v/v). The polar fraction was reconstituted in hexane/isopropanol (9:1, v/v) and re-chromatographed over aminopropyl-substituted silica gel (3 ml of SPE column, 1.0 g of aminopropyl-silica, 25 to 40 μm). The alcohol fraction containing the GDGTs was eluted with 5 ml of hexane/isopropanol (9:1, v/v) and, after drying,

was redissolved in hexane/isopropanol (99:1, v/v) to a final concentration of 6 mg/ml for injection into the High-Performance Liquid Chromatograph with a Mass Spectrometer (HPLC/MS) system.

GDGTs were measured on AGILENT liquid chromatograph coupled to an AGILENT single quadrupole mass spectrometer following the analytical protocol of Hopmans *et al.* (*52*). The HPLC instrument was equipped with an AGILENT HILIC silica column (2.1 × 150 mm; 1.5 µm particle size) and a guard column maintained at 30°C. Detection of archaeal core lipids was achieved by single ion recording of their protonated molecular ions ($[M + H]^+$) and compounds were quantified by integration of peak areas using AGILENT Masshunter software. Calculation of TEX_{86}^H-derived temperatures followed Kim *et al.* (*53*). This temperature calibration has a standard residual error of 2.5°C as shown in (*53*) (fig. S2). Reproducibility upon duplicate measurements showed a relative standard error of < 2% (fig. S2).

Supplementary Materials

The PDF file includes:
Supplementary Text
Table S1
Figs. S1 to S5
Legend for data S1
References

Other Supplementary Material for this manuscript includes the following:
Data S1

REFERENCES AND NOTES

1. D. Hopley, K. E. Parnell, P. J. Isdale, The Great Barrier Reef Marine Park: Dimensions and regional patterns. *Aust. Geogr. Stud.* **27**, 47–66 (1989).
2. World Heritage Convention, Great Barrier Reef—UNESCO World Heritage Centre, World Heritage Convention (2020); https://whc.unesco.org/en/list/154.
3. UNESCO, Belize Barrier Reef Reserve System—UNESCO World Heritage Centre (2014); http://whc.unesco.org/en/list/764.
4. P. J. Davies, P. A. Symonds, D. A. Feary, C. J. Pigram, The evolution of the carbonateplatforms of Northeast Australia, in *Controls on Carbonate Platform and Basin Development* SEPM Society for Sedimentary Geology (1989), pp. 233–258.
5. K. T. Lawrence, T. D. Herbert, Late Quaternary sea-surface temperatures in the western Coral Sea: Implications for the growth of the Australian Great Barrier Reef. *Geology* **33**, 677–680 (2005).
6. D. Ellerton, T. M. Rittenour, J. Shulmeister, A. P. Roberts, G. Miot da Silva, A. Gontz, P. A. Hesp, P. Moss, N. Patton, T. Santini, K. Welsh, X. Zhao, Fraser Island (K'gari) and initiation of the Great Barrier Reef linked by Middle Pleistocene sea-level change. *Nat. Geosci.* **15**, 1017–1026 (2022).
7. N. Dubois, P. Kindler, S. Spezzaferri, S. Coric, The initiation of the southern central Great Barrier Reef: New multiproxy data from Pleistocene distal sediments from the Marion Plateau (NE Australia). *Mar. Geol.* **250**, 223–233 (2008).
8. T. Felis, H. V. McGregor, B. K. Linsley, A. W. Tudhope, M. K. Gagan, A. Suzuki, M. Inoue, A. L. Thomas, T. M. Esat, W. G. Thompson, M. Tiwari, D. C. Potts, M. Mudelsee, Y. Yokoyama, J. M. Webster, Intensification of the meridional temperature gradient in the Great Barrier Reef following the Last Glacial Maximum. *Nat. Commun.* **5**, 4102 (2014).
9. L. D. Brenner, B. K. Linsley, J. M. Webster, D. Potts, T. Felis, M. K. Gagan, M. Inoue, H. McGregor, A. Suzuki, A. Tudhope, T. Esat, A. Thomas, W. Thompson, S. Fallon, M. Humblet, M. Tiwari, Y. Yokoyama, Coral record of younger dryas chronozone warmth on the Great Barrier Reef. *Paleoceanogr. Paleoclimatol.* **35**, e2020PA003962 (2020).
10. M. Hollstein, M. Kienast, A. Lückge, Y. Yokoyama, M. Mohtadi, Sea surface temperatures across the Coral Sea over the last glacial-interglacial cycle. *Paleoceanogr. Paleoclimatol.* **39**, e2023PA004757 (2024).
11. F. Regoli, T. De Garidel-Thoron, K. Tachikawa, Z. Jian, L. Ye, A. W. Droxler, G. Lenoir, M. Crucifix, N. Barbarin, L. Beaufort, Progressive shoaling of the equatorial Pacific thermocline over the last eight glacial periods. *Paleoceanography* **30**, 439–455 (2015).
12. T. Russon, M. Elliot, A. Sadekov, G. Cabioch, T. Corrège, P. De Deckker, The mid-Pleistocene transition in the subtropical southwest Pacific. *Paleoceanography* **26**, PA1211 (2011).
13. M. Laugié, J. Michel, A. Pohl, E. Poli, J. Borgomano, Global distribution of modern shallow-water marine carbonate factories: A spatial model based on environmental parameters. *Sci. Rep.* **9**, 16432 (2019).
14. R. van Woesik, T. Shlesinger, A. G. Grottoli, R. J. Toonen, R. Vega Thurber, M. E. Warner, A. Marie Hulver, L. Chapron, R. H. McLachlan, R. Albright, E. Crandall, T. M. DeCarlo, M. K. Donovan, J. Eirin-Lopez, H. B. Harrison, S. F. Heron, D. Huang, A. Humanes, T. Krueger, J. S. Madin, D. Manzello, L. C. McManus, M. Matz, E. M. Muller, M. Rodriguez-Lanetty, M. Vega-Rodriguez, C. R. Voolstra, J. Zaneveld, Coral-bleaching responses to climate change across biological scales. *Glob. Change Biol.* **28**, 4229–4250 (2022).
15. J. E. N. Vernon, L. M. Devantier, E. Turak, A. L. Green, S. Kininmonth, M. Stafford-Smith, N. Peterson, Delineating the Coral Triangle. *Galaxea J. Coral Reef Stud.* **11**, 91–100 (2009).
16. J. M. Lough, Coral calcification from skeletal records revisited. *Mar. Ecol. Prog. Ser.* **373**, 257–264 (2008).
17. N. S. Jones, A. Ridgwell, E. J. Hendy, Evaluation of coral reef carbonate production models at a global scale. *Biogeosciences* **12**, 1339–1356 (2015).
18. A. R. Isern, J. A. McKenzie, D. A. Feary, The role of sea-surface temperature as a control on carbonate platform development in the western Coral Sea. *Palaeogeogr. Palaeoclimatol. Palaeoecol.* **124**, 247–272 (1996).
19. K. D. Anderson, N. E. Cantin, S. F. Heron, C. Pisapia, M. S. Pratchett, Variation in growth rates of branching corals along Australia's Great Barrier Reef. *Sci. Rep.* **7**, 2920 (2017).
20. J. M. Lough, D. J. Barnes, Environmental controls on growth of the massive coral Porites. *J. Exp. Mar. Biol. Ecol.* **245**, 225–243 (2000).
21. E. Gischler, J. H. Hudson, Holocene tropical reef accretion and lagoon sedimentation: A quantitative approach to the influence of sea-level rise, climate and subsidence (Belize, Maldives, French Polynesia). *Depositional Record* **5**, 515–539 (2019).
22. J. M. Webster, P. J. Davies, Coral variation in two deep drill cores: Significance for the Pleistocene development of the Great Barrier Reef. *Sediment. Geol.* **159**, 61–80 (2003).
23. C. J. R. Braithwaite, L. F. Montaggioni, The Great Barrier Reef: A 700 000 year diagenetic history. *Sedimentology* **56**, 1591–1622 (2009).
24. E. Abbey, J. M. Webster, R. J. Beaman, Geomorphology of submerged reefs on the shelf edge of the Great Barrier Reef: The influence of oscillating Pleistocene sea-levels. *Mar. Geol.* **288**, 61–78 (2011).
25. M. Humblet, J. M. Webster, Coral community changes in the Great Barrier Reef in response to major environmental changes over glacial-interglacial timescales. *Palaeogeogr. Palaeoclimatol. Palaeoecol.* **472**, 216–235 (2017).
26. C. J. R. Braithwaite, H. Dalmasso, M. A. Gilmour, D. D. Harkness, G. M. Henderson, R. L. F. Kay, D. Kroon, L. F. Montaggioni, P. A. Wilson, The Great Barrier Reef: The chronological record from a new borehole. *J. Sediment. Res.* **74**, 298–310 (2004).
27. S. Alpay, "An Investigation of Results from Deep Ocean Drilling off the Northeast Australian Margin," thesis, Carleton University (1996).
28. R. W. Reynolds, N. A. Rayner, T. M. Smith, D. C. Stokes, W. Wang, An improved in situ and satellite SST analysis for climate. *J. Climate* **15**, 1609–1625 (2002).
29. J. M. Webster, J. C. Braga, M. Humblet, D. C. Potts, Y. Iryu, Y. Yokoyama, K. Fujita, R. Bourillot, T. M. Esat, S. Fallon, W. G. Thompson, A. L. Thomas, H. Kan, H. V. McGregor, G. Hinestrosa, S. P. Obrochta, B. C. Lougheed, Response of the Great Barrier Reef to sea-level and environmental changes over the past 30,000 years. *Nat. Geosci.* **11**, 426–432 (2018).
30. T. P. Boyer, H. E. García, R. A. Locarnini, M. M. Zweng, A. V. Mishonov, J. R. Reagan, K. A. Weathers, O. K. Baranova, C. R. Paver, D. Seidov, I. V. Smolyar, World Ocean Atlas 2018, OAA National Centers for Environmental Information. Dataset (2018).
31. L. E. Lisiecki, M. E. Raymo, A Pliocene-Pleistocene stack of 57 globally distributed benthic $\delta^{18}O$ records. *Paleoceanography* **20**, PA1003 (2005).
32. G. H. Haug, K. A. Hughen, D. M. Sigman, L. C. Peterson, U. Rohl, U. Röhl, Southward migration of the intertropical convergence zone through the Holocene. *Science* **293**, 1304–1308 (2001).
33. G. H. Haug, D. M. Sigman, R. Tiedemann, T. F. Pedersen, M. Sarnthein, Onset of permanent stratification in the subarctic Pacific Ocean. *Nature* **401**, 779–782 (1999).
34. Y. G. Zhang, J. Ji, W. Balsam, L. Liu, J. Chen, Mid-Pliocene Asian monsoon intensification and the onset of Northern Hemisphere glaciation. *Geology* **37**, 599–602 (2009).
35. B. Petrick, A. Martínez-García, G. Auer, L. Reuning, A. Auderset, H. Deik, H. Takayanagi, D. De Vleeschouwer, Y. Iryu, G. H. Haug, Glacial Indonesian Throughflow weakening across the Mid-Pleistocene Climatic Transition. *Sci. Rep.* **9**, 16995 (2019).
36. G. Auer, B. Petrick, T. Yoshimura, B. L. Mamo, L. Reuning, H. Takayanagi, D. De Vleeschouwer, A. Martinez-Garcia, Intensified organic carbon burial on the Australian shelf after the Middle Pleistocene transition. *Quat. Sci. Rev.* **262**, 106965 (2021).
37. P. N. DiNezio, J. E. Tierney, B. L. Otto-Bliesner, A. Timmermann, T. Bhattacharya, N. Rosenbloom, E. Brady, Glacial changes in tropical climate amplified by the Indian Ocean. *Sci. Adv.* **4**, eaat9658 (2018).
38. I. Candy, G. R. Coope, J. R. Lee, S. A. Parfitt, R. C. Preece, J. Rose, D. C. Schreve, Pronounced warmth during early Middle Pleistocene interglacials: Investigating the Mid-Brunhes Event in the British terrestrial sequence. *Earth Sci. Rev.* **103**, 183–196 (2010).

39. A. Koutsodendris, J. Pross, R. Zahn, Exceptional Agulhas leakage prolonged interglacial warmth during MIS 11c in Europe. *Paleoceanography* **29**, 1062–1071 (2014).
40. A. W. Droxler, S. J. Jorry, Deglacial origin of barrier reefs along low-latitude mixed siliciclastic and carbonate continental shelf edges. *Ann. Rev. Mar. Sci.* **5**, 165–190 (2013).
41. M. Humblet, D. C. Potts, J. M. Webster, J. C. Braga, Y. Iryu, Y. Yokoyama, R. Bourillot, C. Séard, A. Droxler, K. Fujita, E. Gischler, H. Kan, Late glacial to deglacial variation of coralgal assemblages in the Great Barrier Reef, Australia. *Glob. Planet. Change* **174**, 70–91 (2019).
42. S. E. McIlroy, P. D. Thompson, F. L. Yuan, T. C. Bonebrake, D. M. Baker, Subtropical thermal variation supports persistence of corals but limits productivity of coral reefs. *Proc. R. Soc. B* **286**, 20190882 (2019).
43. N. Santodomingo, W. Renema, K. G. Johnson, Understanding the murky history of the Coral Triangle: Miocene corals and reef habitats in East Kalimantan (Indonesia). *Coral Reefs* **35**, 765–781 (2016).
44. K. L. Sanborn, J. M. Webster, D. Erler, G. E. Webb, M. Salas-Saavedra, Y. Yokoyama, The impact of elevated nutrients on the Holocene evolution of the Great Barrier Reef. *Quat. Sci. Rev.* **332**, 108636 (2024).
45. B. J. Henley, H. V. McGregor, A. D. King, O. Hoegh-Guldberg, A. K. Arzey, D. J. Karoly, J. M. Lough, T. M. DeCarlo, B. K. Linsley, Highest ocean heat in four centuries places Great Barrier Reef in danger. *Nature* **632**, 320–326 (2024).
46. Z. Huang, M. Feng, S. J. Dalton, A. G. Carroll, Marine heatwaves in the Great Barrier Reef and Coral Sea: Their mechanisms and impacts on shallow and mesophotic coral ecosystems. *Sci. Total Environ.* **908**, 168063 (2024).
47. W. F. Precht, R. B. Aronson, Climate flickers and range shifts of reef corals. *Front. Ecol. Environ.* **2**, 307–314 (2004).
48. A. Nakabayashi, T. Yamakita, T. Nakamura, H. Aizawa, Y. F. Kitano, A. Iguchi, H. Yamano, S. Nagai, S. Agostini, K. M. Teshima, N. Yasuda, The potential role of temperate Japanese regions as refugia for the coral *Acropora hyacinthus* in the face of climate change. *Sci. Rep.* **9**, 1892 (2019).
49. D. Lirman, S. Schopmeyer, D. Manzello, L. J. Gramer, W. F. Precht, F. Muller-Karger, K. Banks, B. Barnes, E. Bartels, A. Bourque, J. Byrne, S. Donahue, J. Duquesnel, L. Fisher, D. Gilliam, J. Hendee, M. Johnson, K. Maxwell, E. McDevitt, J. Monty, D. Rueda, R. Ruzicka, S. Thanner, Severe 2010 cold-water event caused unprecedented mortality to corals of the Florida reef tract and reversed previous survivorship patterns. *PLOS ONE* **6**, e23047 (2011).
50. D. R. Easterling, G. A. Meehl, C. Parmesan, S. A. Changnon, T. R. Karl, L. O. Mearns, Climate extremes: Observations, modeling, and impacts. *Science* **289**, 2068–2074 (2000).
51. E. Kodra, K. Steinhaeuser, A. R. Ganguly, Persisting cold extremes under 21st-century warming scenarios. *Geophys. Res. Lett.* **38**, L08705 (2011).
52. E. C. Hopmans, S. Schouten, J. S. Sinninghe Damsté, The effect of improved chromatography on GDGT-based palaeoproxies. *Org. Geochem.* **93**, 1–6 (2016).
53. J.-H. Kim, J. der Meer, S. Schouten, P. Helmke, V. Willmott, F. Sangiorgi, N. Koç, E. C. Hopmans, J. S. S. Damsté, New indices and calibrations derived from the distribution of crenarchaeal isoprenoid tetraetherlipids: Implications for past sea surface temperature reconstructions. *Geochem. et Cosmochim. Acta* **74**, 4639–4654 (2010).
54. E. Kalnay, M. Kanamitsu, R. Kistler, W. Collins, D. Deaven, L. Gandin, M. Iredell, S. Saha, G. White, J. Woollen, Y. Zhu, M. Chelliah, W. Ebisuzaki, W. Higgins, J. Janowiak, K. C. Mo, C. Ropelewski, J. Wang, A. Leetmaa, R. Reynolds, R. Jenne, D. Joseph, The NCEP/NCAR 40-year reanalysis project. *Bull. Am. Meteorol. Soc.* **77**, 437–472 (1996).
55. M. Medina-Elizalde, D. W. Lea, The mid-Pleistocene transition in the tropical Pacific. *Science* **310**, 1009–1012 (2005).
56. Google Earth, Map of the Coral Sea, (2024); https://earth.google.com/web/@-18.6351265,150.3226725,-76.23829286a,1092854.04971972d,35y,0.0599h,0t,0r/data=CgRCAggBOgMKATBCAggASg0I_____ARAA.
57. International Consortium for Great Barrier Reef Drilling, New constraints on the origin of the Australian Great Barrier Reef: Results from an international project of deep coring. *Geology* **29**, 483–486 (2001).
58. J. C. Braga, J. Aguirre, Coralline algae indicate Pleistocene evolution from deep, open platform to outer barrier reef environments in the northern Great Barrier Reef margin. *Coral Reefs* **23**, 547–558 (2004).
59. Y. Yokoyama, J. M. Webster, C. Cotterill, J. C. Braga, L. Jovane, H. Mills, S. Morgan, A. Suzuki, the IODP Expedition 325 Scientists, IODP Expedition 325: Great Barrier Reefs reveals past sea-level, climate and environmental changes since the last ice age. *Sci. Drill.* **12**, 32–45 (2011).
60. T. Russon, M. Elliot, A. Sadekov, G. Cabioch, T. Corrge, P. De Deckker, Inter-hemispheric asymmetry in the early Pleistocene Pacific warm pool. *Geophys. Res. Lett.* **37**, L11601 (2010).
61. S. Schouten, E. C. Hopmans, E. Schefuss, J. S. Sinninghe Damsté, Distributional variations in marine crenarchaeotal membrane lipids: A new tool for reconstructing ancient sea water temperatures? *Earth Planet. Sci. Lett.* **204**, 265–274 (2002).
62. M. W. de Bar, S. W. Rampen, E. C. Hopmans, J. S. Sinninghe Damsté, S. Schouten, Constraining the applicability of organic paleotemperature proxies for the last 90 Myrs. *Org. Geochem.* **128**, 122–136 (2019).
63. D. De Vleeschouwer, M. Peral, M. Marchegiano, A. Fullberg, N. Meinicke, H. Palike, G. Auer, B. Petrick, C. Snoeck, S. Goderis, P. Claeys, Plio-Pleistocene Perth Basin water temperatures and Leeuwin Current dynamics (Indian Ocean) derived from oxygen and clumped-isotope paleothermometry. *Clim. Past* **18**, 1231–1253 (2022).
64. N. Meinicke, M. A. Reimi, A. C. Ravelo, A. N. Meckler, Coupled Mg/Ca and clumped isotope measurements indicate lack of substantial mixed layer cooling in the Western Pacific Warm Pool during the last ~5 million years. *Paleoceanogr Paleoclimatol* **36**, e2020PA004115 (2021).
65. Y. G. Zhang, C. L. Zhang, X.-L. Liu, L. Li, K.-U. Hinrichs, J. E. Noakes, Methane Index: A tetraether archaeal lipid biomarker indicator for detecting the instability of marine gas hydrates. *Earth Planet. Sci. Lett.* **307**, 525–534 (2011).
66. J. W. H. Weijers, S. Schouten, E. C. Hopmans, J. A. J. Geenevasen, O. R. P. David, J. M. Coleman, R. D. Pancost, J. S. Sinninghe Damsté, Membrane lipids of mesophilic anaerobic bacteria thriving in peats have typical archaeal traits. *Environ. Microbiol.* **8**, 648–657 (2006).
67. J. S. Sinninghe Damsté, J. Ossebaar, S. Schouten, D. Verschuren, Distribution of tetraether lipids in the 25-ka sedimentary record of Lake Challa: Extracting reliable TEX86 and MBT/CBT palaeotemperatures from an equatorial African lake. *Quat. Sci. Rev.* **50**, 43–54 (2012).
68. Y. G. Zhang, M. Pagani, Z. Wang, Ring Index: A new strategy to evaluate the integrity of TEX_{86} paleothermometry. *Paleoceanography* **31**, 220–232 (2016).
69. C. Huguet, A. Schimmelmann, R. Thunell, L. J. Lourens, J. S. S. Damste, S. Schouten, A study of the TEX_{86} paleothermometer in the water column and sediments of the Santa Barbara Basin, California. *Paleoceanography* **22**, PA3203 (2007).
70. W. Xiao, Y. Wang, S. Zhou, L. Hu, H. Yang, Y. Xu, Ubiquitous production of branched glycerol dialkyl glycerol tetraethers (brGDGTs) in global marine environments: A new source indicator for brGDGTs. *Biogeosciences* **13**, 5883–5894 (2016).
71. B. Petrick, L. Reuning, G. Auer, Y. Zhang, M. Pfeiffer, L. Schwark, Warm, not cold temperatures contributed to a Late Miocene reef decline in the Coral Sea. *Sci. Rep.* **13**, 4015 (2023).
72. Shipboard Scientific Party, Site 820, in *Proceedings of the Ocean Drilling Program, 133 Initial Reports*, P. J. Davies, J. A. McKenzie, A. Palmer-Julson, et al., Eds. (Ocean Drilling Program, 1991; http://www-odp.tamu.edu/publications/133_IR/VOLUME/CHAPTERS/ir133_13.pdf), pp. 509–568.
73. K. W. R. Taylor, M. Huber, C. J. Hollis, M. T. Hernandez-Sanchez, R. D. Pancost, Re-evaluating modern and palaeogene GDGT distributions: Implications for SST reconstructions. *Glob. Planet. Change* **108**, 158–174 (2013).
74. M. T. Hernández-Sánchez, E. M. S. Woodward, K. W. R. Taylor, G. M. Henderson, R. D. Pancost, Variations in GDGT distributions through the water column in the South East Atlantic Ocean. *Geochim. Cosmochim. Acta* **132**, 337–348 (2014).
75. R. Rattanasriampaipong, Y. G. Zhang, A. Pearson, B. P. Hedlund, S. Zhang, Archaeal lipids trace ecology and evolution of marine ammonia-oxidizing archaea. *Proc. Natl. Acad. Sci. U.S.A.* **119**, e2123193119 (2022).
76. J. O. Grimalt, E. Calvo, C. Pelejero, Sea surface paleotemperature errors in $U^{K'}_{37}$ estimation due to alkenone measurements near the limit of detection. *Paleoceanography* **16**, 226–232 (2001).
77. C. Pelejero, E. Calvo, The upper end of the $U^{K'}_{37}$ temperature calibration revisited. *Geochem. Geophys. Geosyst.* **4**, 1014 (2003).
78. J. E. Tierney, M. P. Tingley, BAYSPLINE: A new calibration for the alkenone paleothermometer. *Paleoceanogr. Paleoclimatol.* **33**, 281–301 (2018).
79. P. K. Swart, The formation of dolomite in sediments from the continental margin of northeastern Queensland, in *Proceedings of the Ocean Drilling Program: Scientific Results* (Ocean Drilling Program, 1993), pp. 513–523.
80. P. K. Swart, Comparisons between the oxygen isotopic composition of pore water and *Globigerinoides ruber* in sediments from Hole 817C, in *Proceedings of the Ocean Drilling Program: Scientific Results* (Ocean Drilling Program, 1993), pp. 481–487.
81. J. E. Tierney, M. P. Tingley, A. Bayesian, A Bayesian, spatially-varying calibration model for the TEX_{86} proxy. *Geochim. Cosmochim. Acta* **127**, 83–106 (2014).
82. F. G. Prahl, L. A. Muehlhausen, D. L. Zahnle, Further evaluation of long-chain alkenones as indicators of paleoceanographic conditions. *Geochim. Cosmochim. Acta* **52**, 2303–2310 (1988).
83. P. J. Müller, G. Kirst, G. Ruhland, I. von Storch, A. Rosell-Melé, Calibration of the alkenone paleotemperature index $U_{37}^{K'}$ based on core-tops from the eastern South Atlantic and the global ocean (60°N-60°S). *Geochim. Cosmochim. Acta* **62**, 1757–1772 (1998).
84. K. T. Lawrence, S. C. Woodard, Past sea surface temperatures as measured by different proxies—A cautionary tale from the late Pliocene. *Paleoceanography* **32**, 318–324 (2017).
85. B. Petrick, E. L. McClymont, K. Littler, A. Rosell-Melé, M. O. Clarkson, M. Maslin, U. Röhl, A. E. Shevenell, R. D. Pancost, Oceanographic and climatic evolution of the southeastern subtropical Atlantic over the last 3.5 Ma. *Earth Planet. Sci. Lett.* **492**, 12–21 (2018).
86. H. Elderfield, P. Ferretti, M. Greaves, S. Crowhurst, I. N. McCave, D. Hodell, A. M. Piotrowski, Evolution of ocean temperature and ice volume through the mid-Pleistocene climate transition. *Science* **337**, 704–709 (2012).

87. K. T. Lawrence, A. Pearson, I. S. Castañeda, C. Ladlow, L. C. Peterson, C. E. Lawrence, Comparison of late Neogene $U^{K'}_{37}$ and TEX_{86} Paleotemperature records from the eastern equatorial Pacific at orbital resolution. *Paleoceanogr. Paleoclimatol.* **35**, e2020PA003858 (2020).
88. S. C. Brassell, Climatic influences on the Paleogene evolution of alkenones. *Paleoceanography* **29**, 255–272 (2014).
89. G. J. M. Versteegh, R. Riegman, J. W. de Leeuw, J. H. F. Jansen, $U_{37}^{K'}$ values for *Isochrysis galbana* as a function of culture temperature, light intensity and nutrient concentrations. *Org. Geochem.* **32**, 785–794 (2001).
90. A. Rosell-Mele, E. McClymont, Biomarkers as paleoceanographic proxies, in *Proxies in Late Cenozoic Paleoceanography*, C. Hillaire-Marcel, A. de Vernal, Eds. (Elsevier, 2007), vol. 1, pp. 441–490.
91. E. L. McClymont, A. Rosell-Melé, J. Giraudeau, C. Pierre, J. M. Lloyd, Alkenone and coccolith records of the mid-Pleistocene in the south-east Atlantic: Implications for the $U_{37}^{K'}$ index and South African climate. *Quat. Sci. Rev.* **24**, 1559–1572 (2005).
92. R. A. Smith, I. S. Castañeda, J. Groeneveld, D. De Vleeschouwer, J. Henderiks, B. A. Christensen, W. Renema, G. Auer, K. Bogus, S. J. Gallagher, C. S. Fulthorpe, Retracted: Plio–Pleistocene Indonesian Throughflow variability drove Eastern Indian Ocean sea surface temperatures. *Paleoceanogr. Paleoclimatol.* **35**, e2020PA003872 (2020).
93. Y. Rosenthal, S. Bova, X. Zhou, A user guide for choosing planktic foraminiferal Mg/Ca-temperature calibrations. *Paleoceanogr. Paleoclimatol.* **37**, e2022PA00413 (2022).
94. R. A. Locarnini, A. V. Mishonov, O. K. Baranova, T. P. Boyer, M. M. Zweng, H. E. Garcia, J. R. Reagan, D. Seidov, K. W. Weathers, C. R. Paver, I. V. Smolyar, World Ocean Atlas. **1**, 52 (2019).
95. W. Wei, S. Gartner, Neogene calcareous nannofossils from sites 811 and 819 through 825, offshore Northeastern Australia, in *Proceedings of the Ocean Drilling Program: Scientific Results* (Ocean Drilling Program, 1993), vol. 133; https://doi.org/10.2973/odp.proc.sr.133.216.1993.
96. C. E. Barton, S. K. Omarzai, I. Alexer, F. Peerdeman, D. McNeill, Magnetic stratigraphy and characterization of sediments from the Northeast Margin of Australia and their relationship to environmental change during the Quaternary, in *Proceedings of the Ocean Drilling Program: Scientific Results* (Ocean Drilling Program, 1993; http://www-odp.tamu.edu/publications/133_SR/VOLUME/CHAPTERS/sr133_49.pdf).
97. P. T. Moss, G. B. Dunbar, Z. Thomas, C. Turney, A. P. Kershaw, G. E. Jacobsen, A 60 000-year record of environmental change for the Wet Tropics of north-eastern Australia based on the ODP 820 marine core. *J. Quat. Sci.* **32**, 704–716 (2017).
98. F. M. Peerdeman, P. J. Davies, A. R. Chivas, The stable oxygen isotope signal in shallow-water, upper-slope sediments off the Great Barrier Reef (Hole 820A), in *Proceedings of the Ocean Drilling Program: Scientific Results* (Ocean Drilling Program, 1993), pp. 163–173.
99. N. J. Shackleton, M. A. Hall, J. Line, C. Shuxi, Carbon isotope data in core V19-30 confirm reduced carbon dioxide concentration in the ice age atmosphere. *Nature* **306**, 319–322 (1983).
100. F. M. Gradstein, J. G. Ogg, The chronostratigraphic scale. *Geologic Time Scale 2020* **1**, 21–32 (2020).
101. A. Rosell-Melé, E. Bard, F. Rostek, C. Sonzogni, K. C. Emeis, J. O. Grimalt, C. Pelejero, P. Müller, R. Schneider, I. Bouloubassi, L. Mejanelle, B. Epstein, J. Quinn, K. Fahl, A. Fluegge, K. Freeman, R. D. Pancost, M. Goñi, D. Hartz, U. Güntner, J. Rullkötter, S. Hellebust, T. Herbert, M. Ikehara, K. Kawamura, N. Ohkouchi, Y. Ternois, R. Ishiwatari, F. Kenig, J. de Leeuw, G. Versteegh, S. Lehman, J. Sachs, F. Prahl, J. F. Rontani, T. Blanz, D. Schulz-Bull, K. Sawada, E. Sikes, J. K. Volkman, S. Wakeham, Precision of the current methods to measure the alkenone proxy $U_{37}^{K'}$ and absolute alkenone abundance in sediments: Results of an interlaboratory comparison study. *Geochem. Geophys. Geosyst.* **2**, 1046 (2001).

Acknowledgments: We would like to thank the participants on ODP Expedition 133 for recovering the core and providing the initial data. This is especially true of the late J. McKenzie and D. Kroon, who both sailed on the initial expedition. We thank the IODP core repository at Kochi for providing the samples. IODP has provided important support for this project. We also want to thank A. Droxler and F. Regoli for providing their data. **Funding:** This project was funded by a grant from the Deutsche Forschungsgemeinschaft (DFG)—project no. 447611930 for B.P. and by the Deutsche Forschungsgemeinschaft (DFG, German Research Foundation)—project nos. 468545267 and 468545728 for M.P. and SPP 2299/project number 441832482 for M.P. **Author contributions:** All authors approved the manuscript and agreed to its submission. All authors discussed the results and provided input to the final version of the manuscript. B.P., L.R., and L.S. designed the study. L.S. performed the biomarker analysis in his laboratory based on samples selected by B.P. B.P. and L.S. interpreted the biomarker data. G.A. helped refine the age model by investigating nannofossils. A.A. helped with the interpretation of the biomarkers and the generation of figures. M.P. and L.R. helped with understanding reef dynamics. Last, B.P., G.A., L.R., L.S., M.P., and A.A. provided vital feedback on the article and helped with the editing. **Competing interests:** The authors declare that they have no competing interests. **Data and materials availability:** All data needed to evaluate the conclusions in the paper are present in the paper and/or the Supplementary Materials.

Submitted 22 January 2024
Accepted 31 October 2024
Published 4 December 2024
10.1126/sciadv.ado2058